



Review

Virtual Dissection: Emerging as the Gold Standard of Analyzing Living Heart Anatomy

Justin T. Tretter ^{1,2}, Saurabh Kumar Gupta ³, Yu Izawa ⁴, Tatsuya Nishii ⁵ and Shumpei Mori ^{6,*}

¹ Heart Institute, Cincinnati Children's Hospital Medical Center, Cincinnati, OH 45229, USA; justin.tretter@cchmc.org

² Department of Pediatrics, University of Cincinnati College of Medicine, Cincinnati, OH 45229, USA

³ Department of Cardiology, All India Institute of Medical Sciences, New Delhi 110029, India; drsaurabhmd@gmail.com

⁴ Division of Cardiovascular Medicine, Department of Internal Medicine, Kobe University Graduate School of Medicine, Kobe, Hyogo 650-0017, Japan; u.izawa@gmail.com

⁵ Department of Radiology, National Cerebral and Cardiovascular Center, Suita, Osaka 564-8565, Japan; ttsynishii@ncvc.go.jp

⁶ UCLA Cardiac Arrhythmia Center, UCLA Health System, David Geffen School of Medicine at UCLA, Los Angeles, CA 90095, USA

* Correspondence: shumpei@g.ucla.edu; Tel.: +310-794-1717; Fax: +310-794-6492

Academic Editors: Deborah Henderson and Nigel Brown

Received: 14 July 2020; Accepted: 10 August 2020; Published: 12 August 2020



Abstract: Traditionally, gross cardiac anatomy has been described mainly based on the findings in the dissection suite. Analyses of heart specimens have contributed immensely towards building a fundamental knowledge of cardiac anatomy. However, there are limitations in analyzing the autopsied heart removed from the thorax. Three-dimensional imaging allows visualization of the blood-filled heart in vivo in attitudinally appropriate fashion. This is of paramount importance for not only demonstration of cardiac anatomy for educational purposes, but also for the detailed anatomical evaluation in patients with acquired and congenital heart disease. In this review, we discuss the advantages of three-dimensional imaging, specifically focusing on virtual dissection, a volume rendering-based reconstruction technique using computed tomographic data. We highlight examples of three-dimensional imaging in both education and guiding patient management.

Keywords: cardiac anatomy; computed tomography; congenital heart disease; three-dimensional imaging; virtual dissection; volume rendering

1. Introduction

The modern understanding of cardiac anatomy is incomplete without referencing the works of Professor Robert H. Anderson. He continues to be a pillar to which our knowledge of cardiac anatomy in both normal as well as malformed hearts is supported. During his long illustrious career, he has enriched the field of cardiac development and anatomy, the latter of which has largely depended on analysis of heart specimens. The autopsy-based analyses, however, have inherent disadvantages of loss of in vivo blood-filled shape and attitudinally appropriate relationship to surrounding structures. Besides, delineation of cardiac anatomy mandates dissection, which results in deformation and permanent loss of its original state.

Modern computed tomography scanners acquire high-resolution datasets. Simultaneous improvement in computational capabilities now permits high-quality three-dimensional reconstruction of computed tomographic datasets. The three-dimensional reconstructions, particularly when achieved

by volume rendering, permit visualization of cardiac anatomy equivalent to the dissection of heart specimens with the additional benefit of viewing in attitudinally appropriate orientation. Such dissection performed virtually has an added advantage of evaluating cardiac anatomy *in vivo*. Furthermore, the feasibility of reconstructing in any plane relevant to the cardiologist, radiologist or surgeon makes virtual dissection an ideal tool for education and clinical decision making. The ease and accuracy of cardiac anatomy using virtual dissection has prompted Professor Anderson to consider it as the gold standard for analysis of cardiac anatomy in living patients [1–3]. We are honored to contribute to this special issue of the journal, recognizing the monumental contributions that Professor Anderson has made to the field of cardiovascular medicine. In this review, we discuss the advantages and applications of volume-rendered images, specifically focusing on virtual dissection, in understanding patient-specific cardiac anatomy.

2. The Concept of Three-Dimensional Imaging Using the Volume-Rendering Method

Recent advances in visualization have permitted much needed three-dimensional reconstruction of datasets obtained from computed tomography and magnetic resonance imaging. Although commonly performed using commercial software packages, three-dimensional reconstruction can also be achieved using free open-source software [4–8]. These software are being increasingly used in clinical practice for diagnosis as well as to guide transcatheter and surgical intervention [9–13]. Some of these software have additional capability for creating and modifying the three-dimensional data to provide the appropriate file format for three-dimensional printing and various forms of extended reality [14,15]. Irrespective of the software and the visualization technique (virtual model on a monitor, printed model, or augmented/virtual reality), the general concept of three-dimensional imaging is the same in the regard that all three-dimensional visualization techniques rely on differential visualization of each iso- or anisotropic image voxel based on its attenuation density (computed tomography), signal intensity (magnetic resonance imaging), or intensity of echocardiographic signal (three-dimensional ultrasound). If a phasic dataset is obtained, four-dimensional images with time-dependent change in the cardiac anatomy can also be demonstrated (Supplementary Movies 1 and 2).

Commonly, contrast enhancement is used for detailed cardiac evaluation to visualize the chambers, vessels, and/or coronary arteries. When the contrast agent is used, it is the enhanced chamber and/or the lumen of these vessels that are usually the focus of reconstruction (Figures 1 and 2). We call this volume-rendering blood pool imaging as endocast images [1,16,17]. This is analogous to conventional die casting used for the dissected heart to create molds [18].

In this material, we mainly focused on the computed tomographic images as the spatial resolution of clinical datasets is commonly superior to that obtained from cardiac magnetic resonance imaging. However, three- or four-dimensional analysis is also feasible for datasets obtained from magnetic resonance imaging, which have advantages in its non-invasiveness, temporal resolution, tissue characterization, perfusion analysis, and flow analysis [19,20].

Virtual dissection is nothing but a modification of the volume-rendering technique wherein the focus is shifted to the walls of the cardiac chambers and vessels. While endocast images can be extremely useful, especially when visualizing the great vessels and their relationships to the other intrathoracic structures or relating to angiographic imaging, they become less informative when aiming to understand the detailed intracardiac anatomy and how this relates to the proximal great vessels. It is often the walls, septums, and valves of the chambers and/or vessels which are targeted for transcatheter or surgical intervention [17], information which can be demonstrated in exquisite detail by virtual dissection [21–25]. In this technique, the enhanced chamber is virtually removed from the original datasets by the process of manual thresholding. The non-enhanced walls, septums, and valves are then visualized to produce images similar to real dissection.

Depending on the interest of visualization, reconstruction using the volume-rendering method requires a combination of various concepts of imaging (Figures 1 and 2).

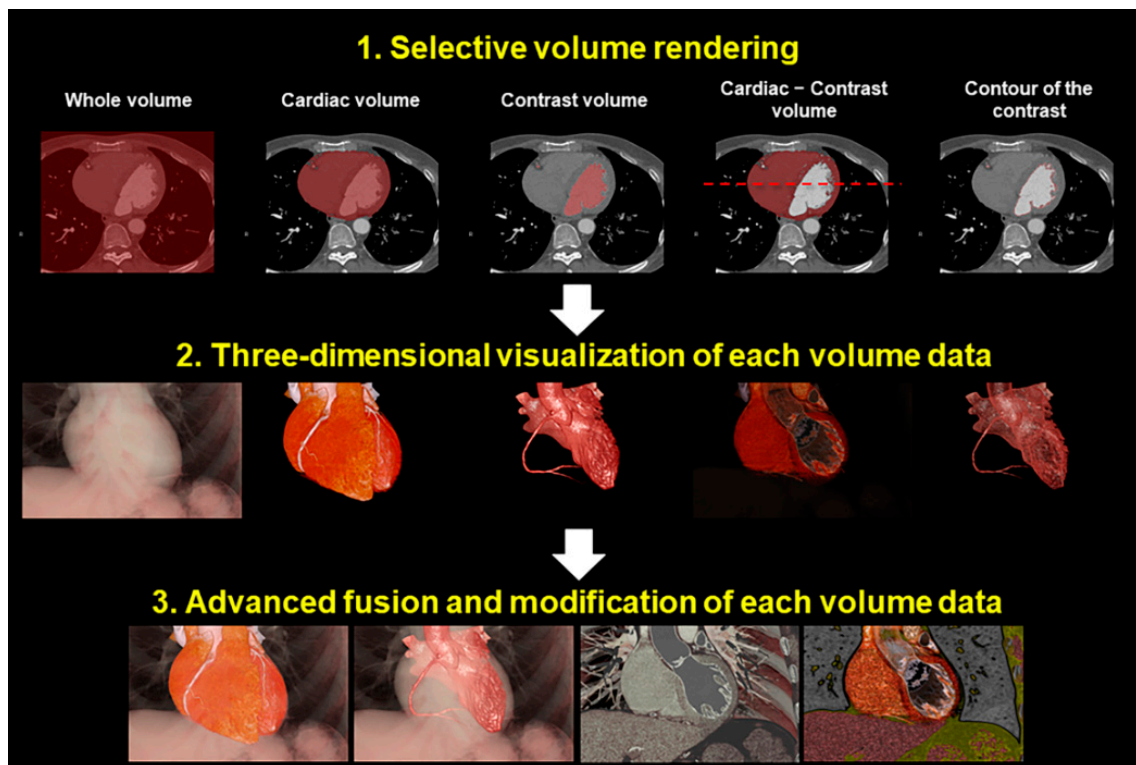


Figure 1. Concept of the image reconstruction. Each volume of interest can be reconstructed separately and can be merged at the reconstructors’ disposal.

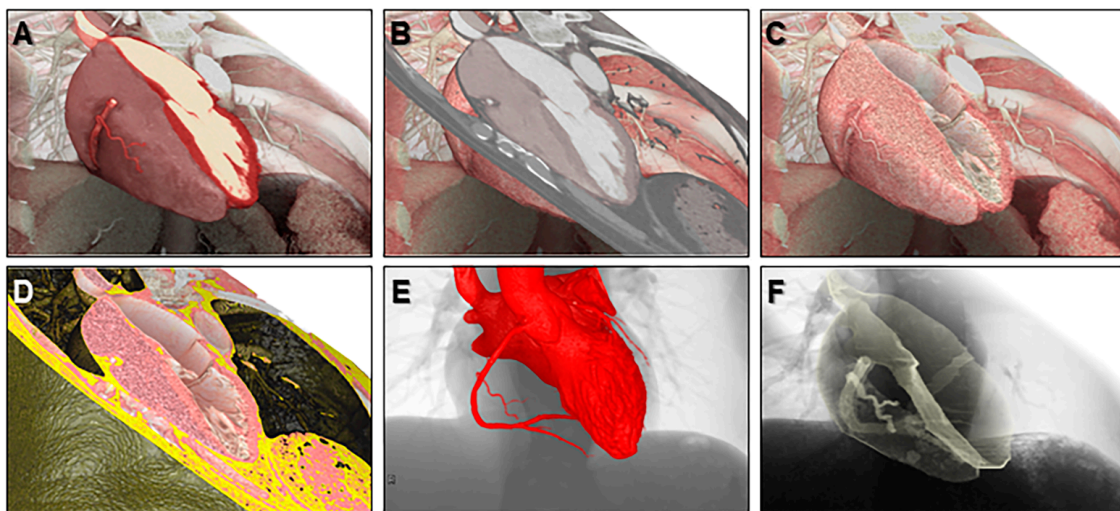


Figure 2. Representative various volume-rendered images reconstructed from a single dataset. We call these volume-rendering techniques 2.5-dimensional imaging (A,B), virtual dissection imaging (C,D), endocast imaging (E), and shell imaging (F).

3. The Advantage of the Virtual Dissection Compared to Conventional Real Dissection

The main advantage of virtual dissection from computed tomographic datasets is that it can provide a high-resolution image of the blood-filled heart without removing it from the thorax (Figure 3). Unlike dissection of the heart specimens, the cut planes during virtual dissection are not fixed and are practically unlimited. Almost any view can be recreated for optimal visualization of the structures of interest as per the need. Each voxel retains its three-dimensional spatial coordinate, allowing the reconstructed image to show the details of living heart anatomy in attitudinally appropriated

fashion [1]. In other words, the right, left, superior, inferior, anterior, and posterior directions are precisely demonstrated, allowing for accurate anatomical education and understanding. This is particularly important in providing relative orientation of cardiac structures with surrounding structures, including the esophagus, trachea and bronchi, lungs, diaphragm, nerves, vertebral column, and thorax itself [1]. Historically, the nomenclature of cardiac anatomy was based on describing the heart in the Valentine position, with the autopsied heart removed from the chest and placed on its apex. While much of this attitudinally incorrect nomenclature has been engrained in the cardiovascular fields, this creates misunderstanding and ambiguity when assessing various cardiovascular structures from common imaging modalities (i.e., angiography, cardiac magnetic resonance and computed tomography, etc.) or by intraoperative assessment with the heart in vivo [1,26,27]. Virtual dissection, on the other hand, by permitting constant guidance about relative orientation of the heart enables a similar attitudinally correct understanding of the in vivo cardiac anatomy by all members of the medical team. Virtual dissection also avoids the risk of being exposed by the potentially toxic fixatives used for specimen preservation, such as formalin. For these reasons, we believe the technique of virtual dissection from computed tomographic datasets has in many ways surpassed analysis of the autopsied heart as the gold standard for understanding detailed cardiac anatomy.

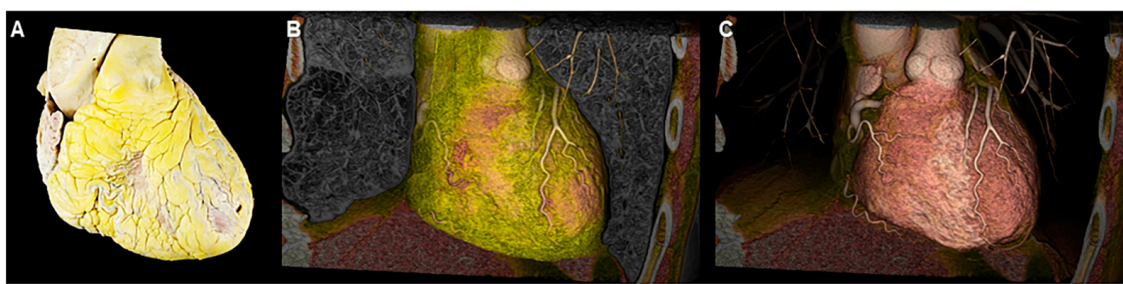


Figure 3. Real dissection (A) and virtual dissection images (B,C). When using virtual dissection images, attitudinal relationships with surrounding structures are maintained with easy modification on images to effectively show the structural anatomy of interest.

4. Educational Implication of the Three-Dimensional Living Heart Anatomy

It is well understood that “form begets function”. Therefore, it is not surprising that the foundation of medical education often begins with instruction in anatomy followed by (patho)physiology. While medical students are taught cardiac anatomy in their first years of medical education, supplemented by cadaveric dissection and inspection, the cardiology and cardiothoracic surgery trainees are often starved of such experiences. This relates to several factors, including the scarcity of preserved heart archives, competing educational requirements in a relatively limited time, and demanding clinical schedules [28–30]. So as to keep and improve the quality of anatomical knowledge, dissection-based teaching alone during medical school has to be complemented with newer teaching/learning methods, based on clinical imaging including computed tomography and magnetic resonance imaging [31–33]. Many cardiology trainees expand upon their knowledge in basic cardiac anatomy by interpretation of two-dimensional imaging modalities, primarily echocardiography. Assessing such a complex three-dimensional organ by two-dimensional means with a narrow field of view is fraught with error [34]. Education in cardiac anatomy using three-dimensional reconstructions has many advantages. There has been interest in using three-dimensional printed models for education albeit with the limitations of availability and costs. On most occasions, the assessment using printed models is also restricted to a singular plane of dissection [35]. Furthermore, similar to the heart specimens, freedom of moving the printed model extracted out of the chest cavity makes the assessment prone to errors. An unnatural tactile feeling of printed models also falls short of the real heart.

While three-dimensional imaging lacks the tactile advantage of the printed model of the heart, an excellent demonstration of cardiac anatomy in attitudinally appropriate orientation makes up for this deficiency to a large extent. Three-dimensional imaging has the potential to serve as the mainstay of imparting knowledge of cardiac anatomy in the absence of heart specimens [1]. Even at centers with a well-maintained archive of heart specimens, virtual dissection has a complementary role in educating students and health professionals. The ease of storing computed tomographic datasets in electronic format with the feasibility of creating endocast and/or virtual dissection images at any time practically immortalizes the anatomic details of any patient (Figures 4–7) [35]. The electronic format also eliminates problems related to sharing of knowledge across institutions which is severely restricted with the use of heart specimens. Figure 8 shows the representative volume-rendered images usually used during routine educational lectures to show the three-dimensional relationship of each anatomical structure in the thorax.

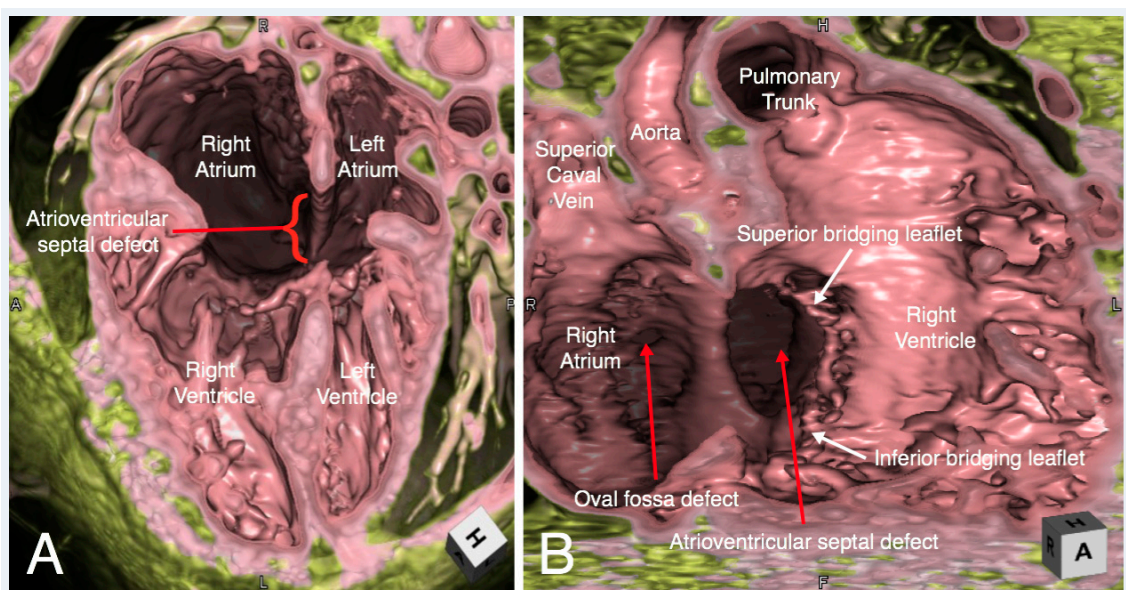


Figure 4. Virtual dissection of an atrioventricular septal defect in four-chamber (Panel A) and right anterior oblique (Panel B) planes. In the right anterior oblique plane (Panel B) the superior and inferior bridging leaflets are seen to have chordal attachments to the crest of the muscular interventricular septum, with small ventricular level shunting between the chordae. There is a large atrial component to the defect. There is additionally a small oval fossa defect.

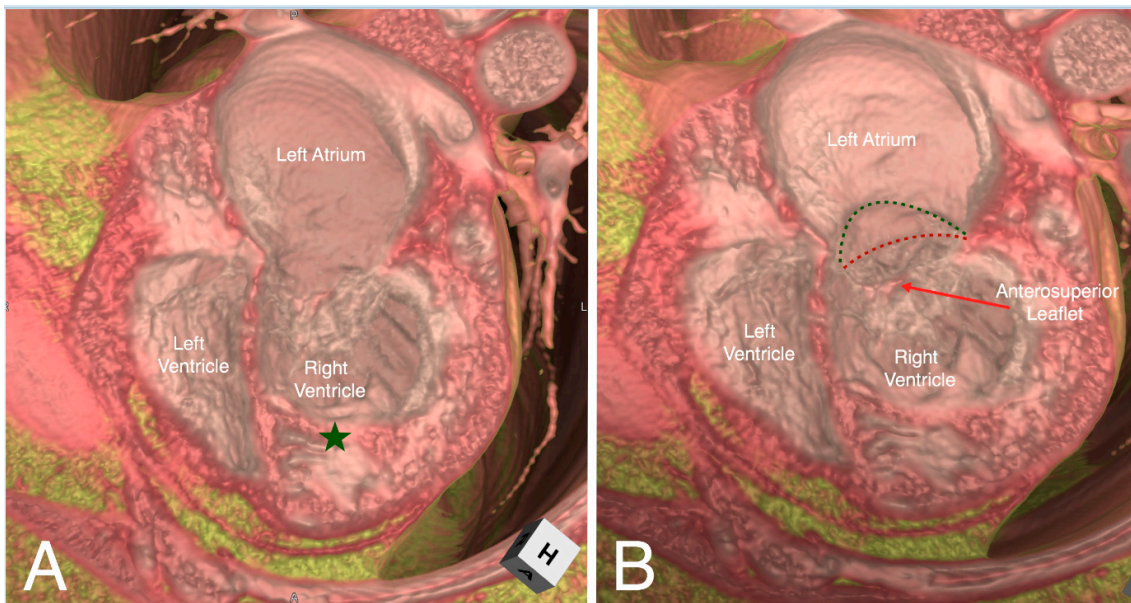


Figure 5. Virtual dissection of a patient with congenitally corrected transposition in a four-chamber plane demonstrating discordant atrioventricular connections with left-hand ventricular topology (Panel A). The moderator band (green star) and septal attachments of the left-sided atrioventricular valve identifies the left-sided ventricle as the morphological right ventricle. Tilting the dissected heart anteriorly and superiorly (Panel B), the hinge points of the septal and inferior tricuspid leaflets (red dashed line) are displaced inferiorly (the green dashed line represents its normal attachment points).

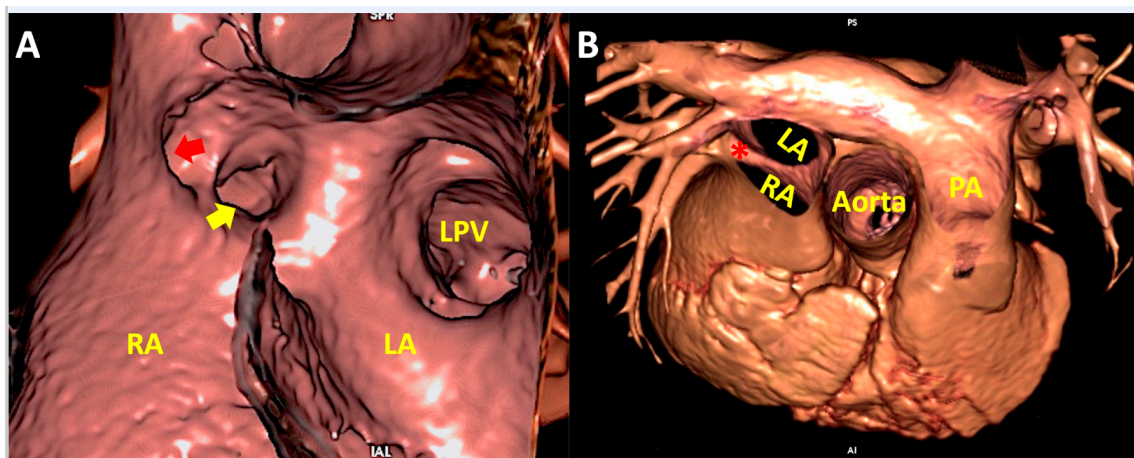


Figure 6. Virtual dissection of a superior sinus venosus interatrial communication in left anterior oblique projection (Panel A) and as viewed from the superior direction (Panel B). Panel A shows extrasseptal location of the defect with anomalous connection of right superior pulmonary vein (red arrow) having retained connection to the left atrium. The right inferior pulmonary vein (yellow arrow) and left pulmonary veins connect normally to the left atrium. Panel B shows overriding of the superior caval vein on the atrial septum (*) when viewed from above. LA—left atrium; LPV—left pulmonary veins; PA—pulmonary artery; RA—right atrium.

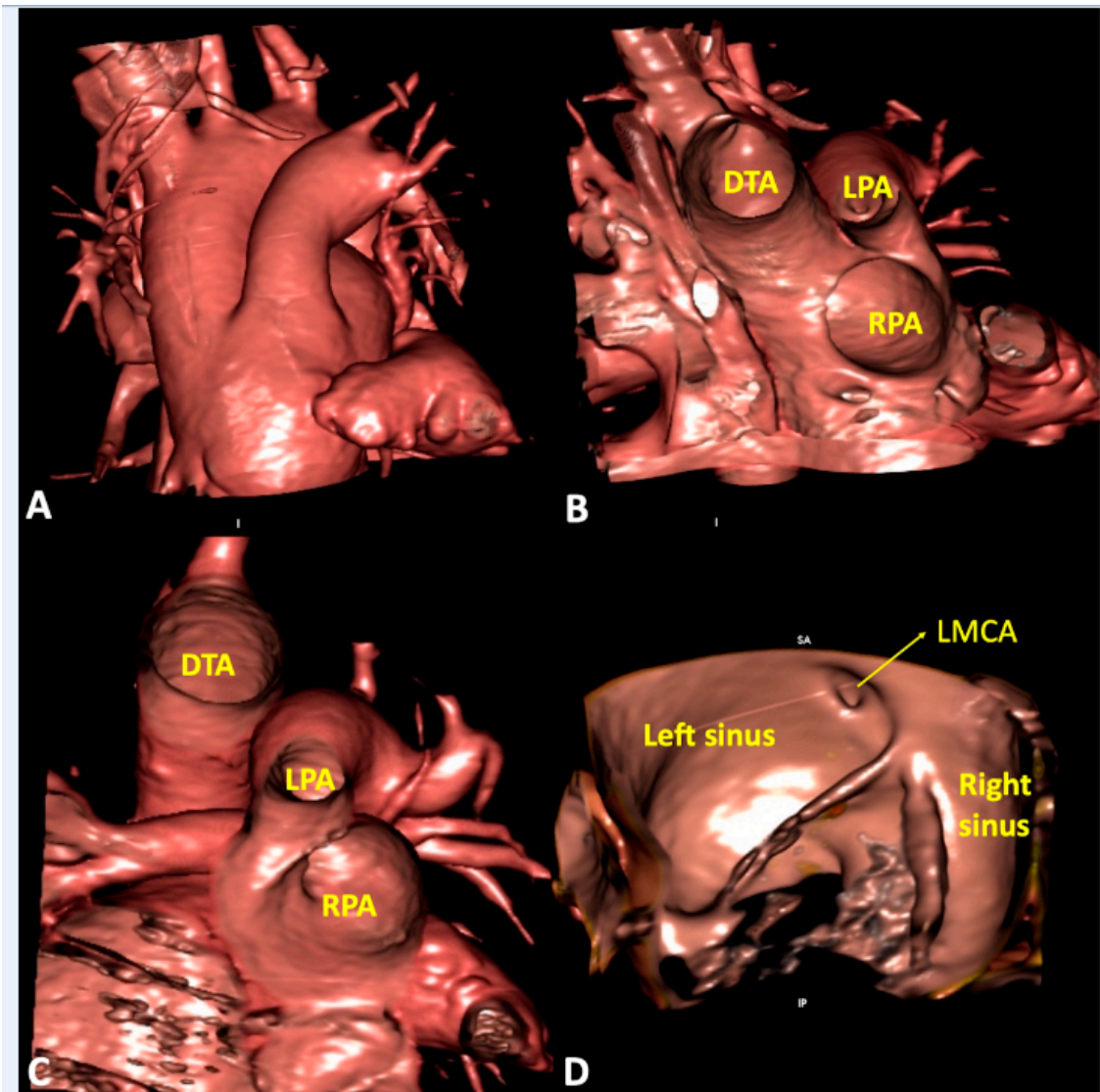


Figure 7. Virtual dissection of patients with common arterial trunk. (Panel A and B) from the same patient shows how it is difficult to clarify common versus separate origin of left and right pulmonary artery based on the external appearance (Panel A). The internal virtual dissection view (Panel B), on the other hand, clearly demonstrates separate origin of the pulmonary arteries. (Panel C) demonstrates crossed pulmonary arteries with the origin of the right pulmonary artery positioned to the left of the left pulmonary artery. (Panel D) shows juxtacommissural origin of left main coronary artery in a patient with bisinusate truncal valve. DTA—descending thoracic aorta; LMCA—left main coronary artery; LPA—left pulmonary artery; RPA—right pulmonary artery.

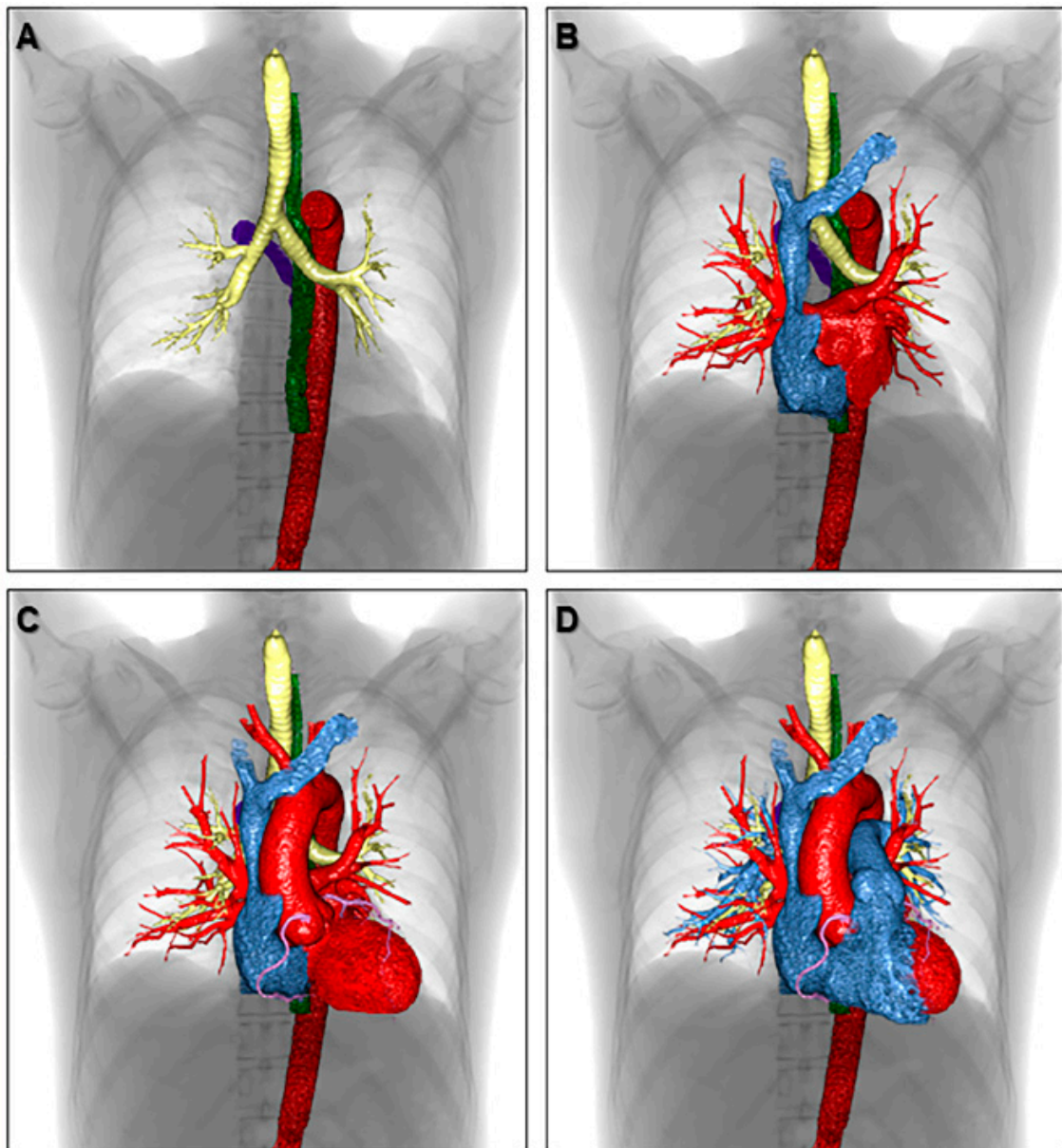


Figure 8. Volume-rendered images showing the three-dimensional relationship of each anatomical structure in the thorax. The azygos vein (purple), descending aorta (red), esophagus (green), trachea, and bronchi (yellow) are shown in panel (A). Both atria are added in panel (B). The left ventricle, aortic root, ascending aorta, aortic arch, and coronary artery are added in panel (C). The right ventricle, pulmonary root, pulmonary trunk, and pulmonary arteries are reconstructed in panel (D) to finalize the components of cardiac silhouette.

5. Clinical Implication in Acquired Heart Disease with Representative Cases

For educational and diagnostic purposes related to the heart, it is not always sufficient to understand only the cardiac anatomy. Often, it is more important to clarify relationships with the adjacent structures in the thoracic cavity [36–38]. Volume-rendered images are useful to relate to abnormal findings in chest radiography in individual cases (Figure 9).

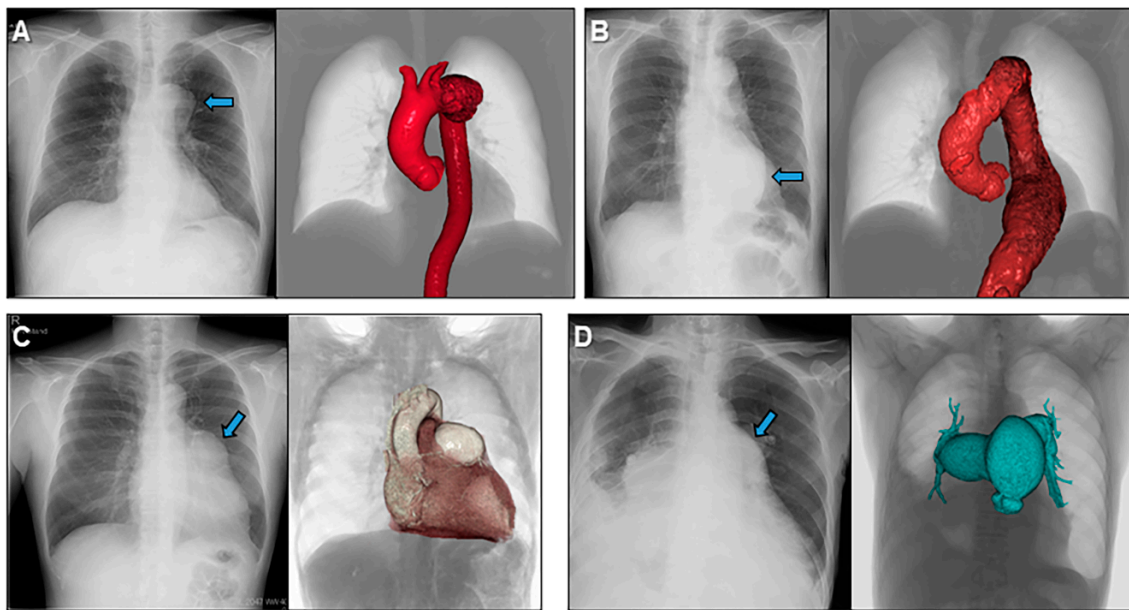


Figure 9. Volume-rendered images to understand abnormal chest radiographies showing a case with aneurysms of the aortic arch (A), descending aorta (B), left coronary artery (C), and pulmonary trunk and pulmonary arteries (D).

For more specific purposes, volume-rendered images, involving both endocast and virtual dissection images, can be also used to educate fluoroscopic anatomy to cardiac interventionists and electrophysiologists as their procedures are commonly performed under fluoroscopic guidance and with angiography (Figure 10). Virtual simulation of the invasive procedure, including electrophysiological study (Figure 11), biventricular pacing [39], radiofrequency catheter ablation, and His-bundle pacing are also feasible. Image demonstration from the surgeon’s view, as well as virtual simulation of the cardiac surgery in preoperative fashion is also feasible with stereoscopic presentation (Figure 12) [40].

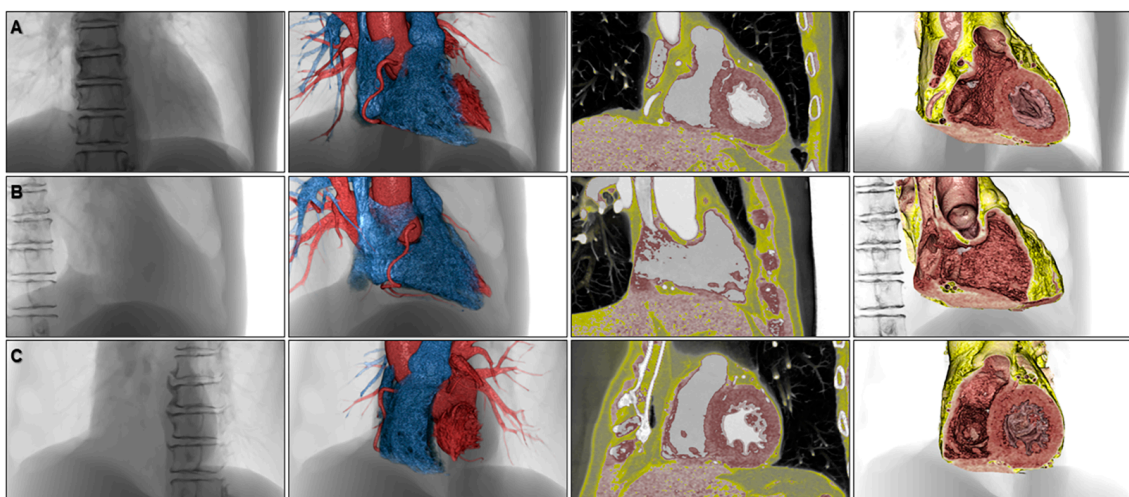


Figure 10. Volume-rendered images to appreciate fluoroscopic anatomy viewed from the frontal (A), right anterior oblique (B), and left anterior oblique (C) directions. The left panels, second left panels, second right panels, and right panels show fluoroscopy-like volume-rendered images, endocast images, 2.5-dimensional images, and virtual dissection images, respectively.

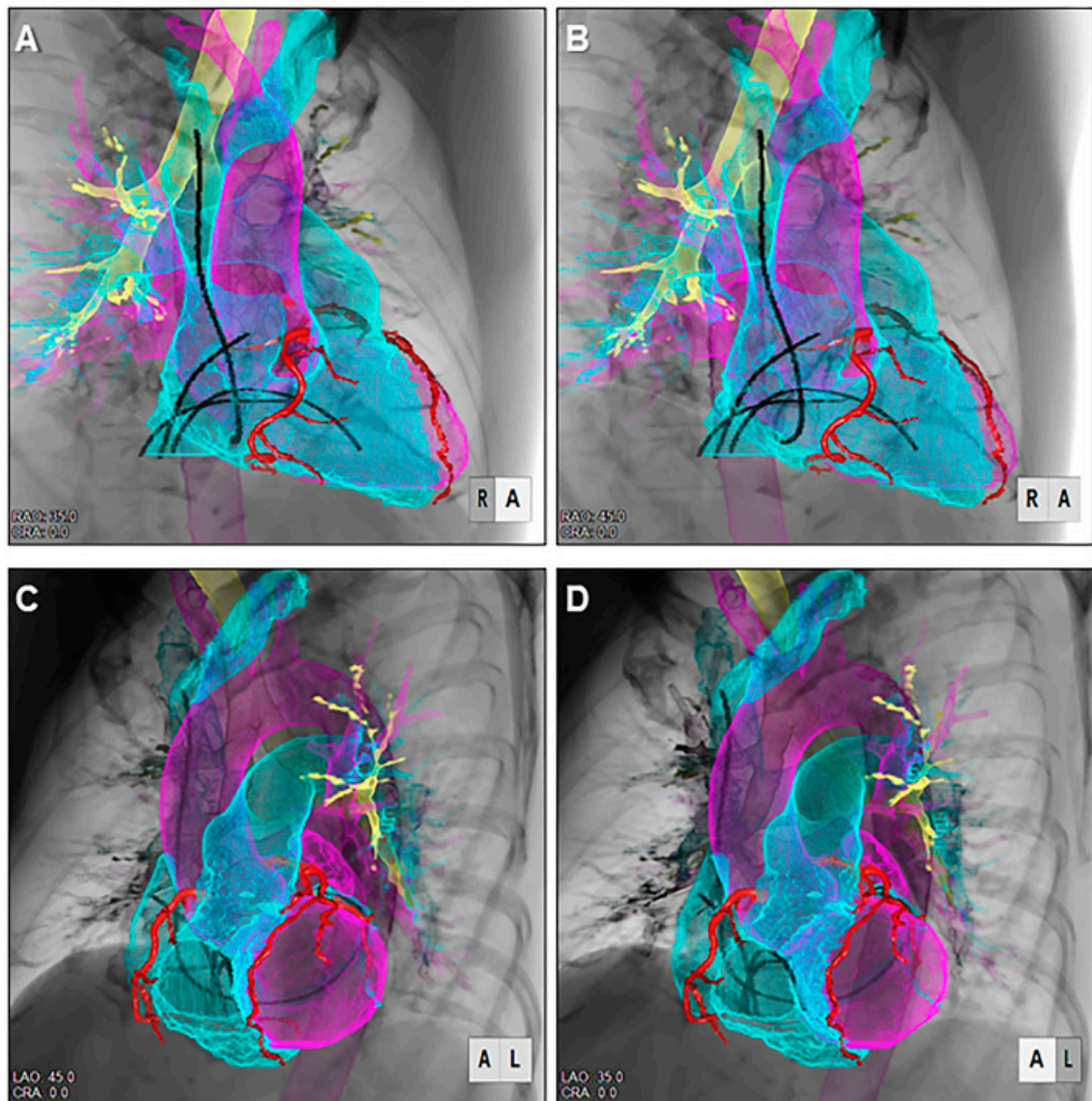


Figure 11. Stereoscopic displays (cross-eyed method) of virtual electrophysiologic catheters placed within the heart reconstructed using shell-imaging technique viewed from the right anterior oblique (A,B) and left anterior oblique (C,D) directions.

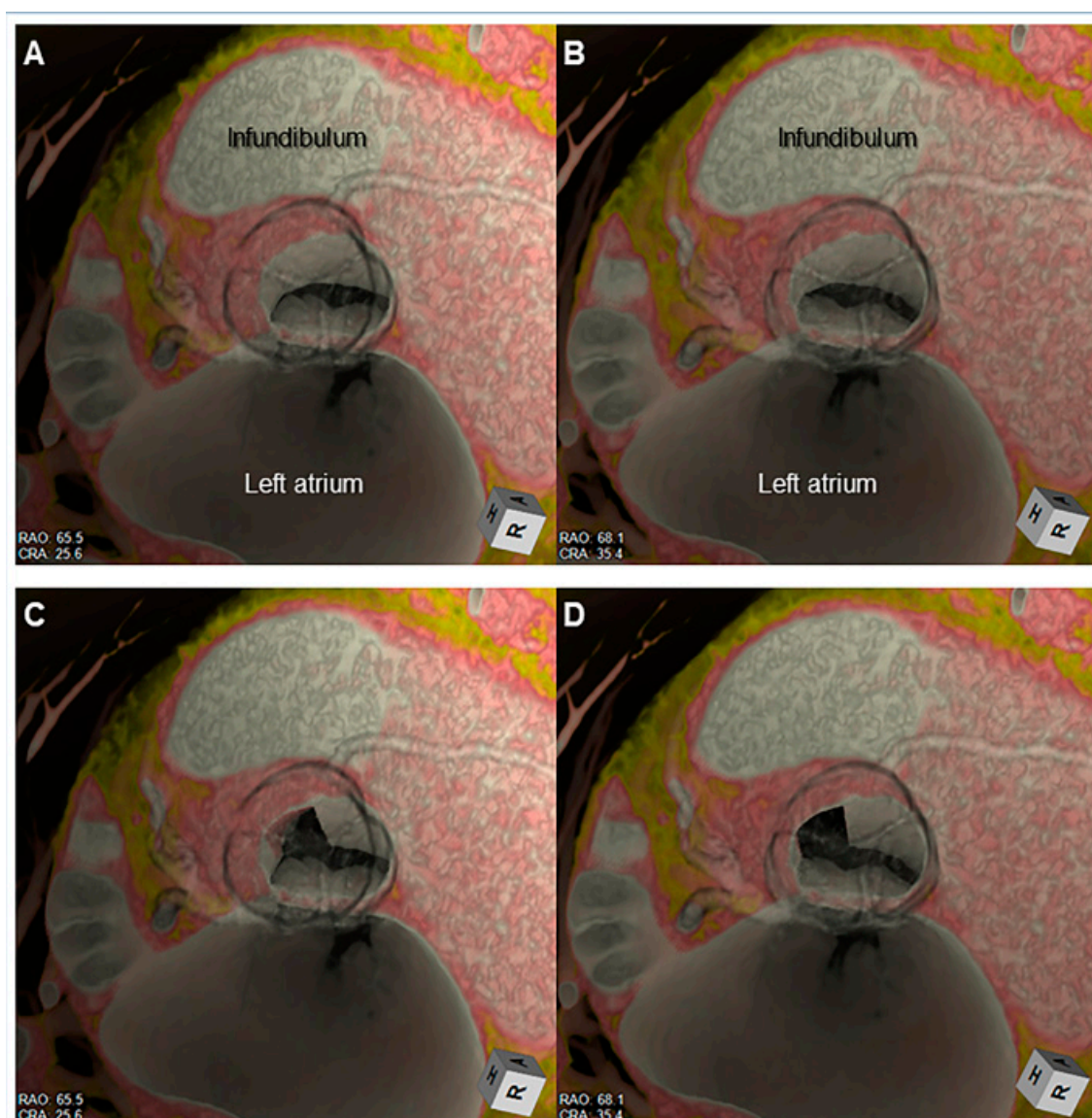


Figure 12. Stereoscopic displays (cross-eyed method) of virtual dissection images demonstrated from the surgeon's view show presurgical virtual simulation of the Morrow's septal myectomy. The hypertrophied septal myocardium located apical to the bottom of the right coronary aortic sinus (A,B) is virtually resected at its left half (C,D).

6. Clinical Implication in Congenital Heart Disease with Representative Cases

Similar applications of three-dimensional reconstructions can be applied towards congenital heart disease. This includes not only in the evaluation of unrepaired congenital heart disease which may involve complex abnormal three-dimensional relationships of chambers and vessels, deficiencies in septation, or abnormalities of atrioventricular or semilunar valves but also in the evaluation of their repaired and palliated forms. A combination of both endocast and virtual dissection images is often beneficial to provide a comprehensive three-dimensional understanding. There is increasing application towards the adult congenital population, given the complexity of evaluating many of their repaired and palliated lesions as well as the common scenario of poor acoustic windows limiting complete echocardiographic evaluation [41].

In addition to cases demonstrated in Figures 4–7, examples of three-dimensional images to guide interventional and surgical management in the congenital heart disease population are illustrated in the following:

- Relationship of the great arteries to an interventricular communication in the setting of double outlet right ventricle for surgical planning (Figure 13);
- Unicuspid aortic valve for surgical repair planning (Figure 14, Supplementary Movie 2);
- Obstruction in surgically constructed pulmonary venous baffles for surgical planning (Figure 15) [16];
- Right ventricular outflow tract obstruction in repaired tetralogy of Fallot to guide transcatheter pulmonary valve replacement (Figure 16).

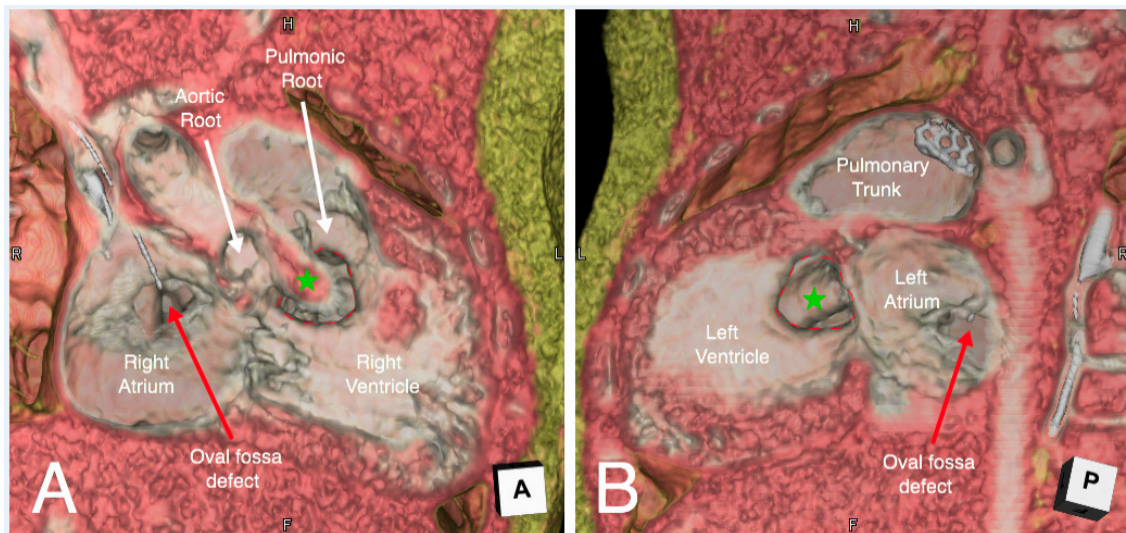


Figure 13. Virtual dissection of a patient with double outlet right ventricle with the interventricular communication (red dashed line) viewed from the right (Panel A) and left side (Panel B). The interventricular communication is doubly committed, bisected by the prominent outlet septum (green star). However, the potential pathway to the relatively larger pulmonary root is larger than that to the small aortic root with subaortic narrowing. There is a stent within the patent arterial duct seen entering the distal pulmonary trunk in this patient with a hypoplastic transverse aortic arch, coarctation of the aorta and ductal-dependent systemic arterial blood flow.

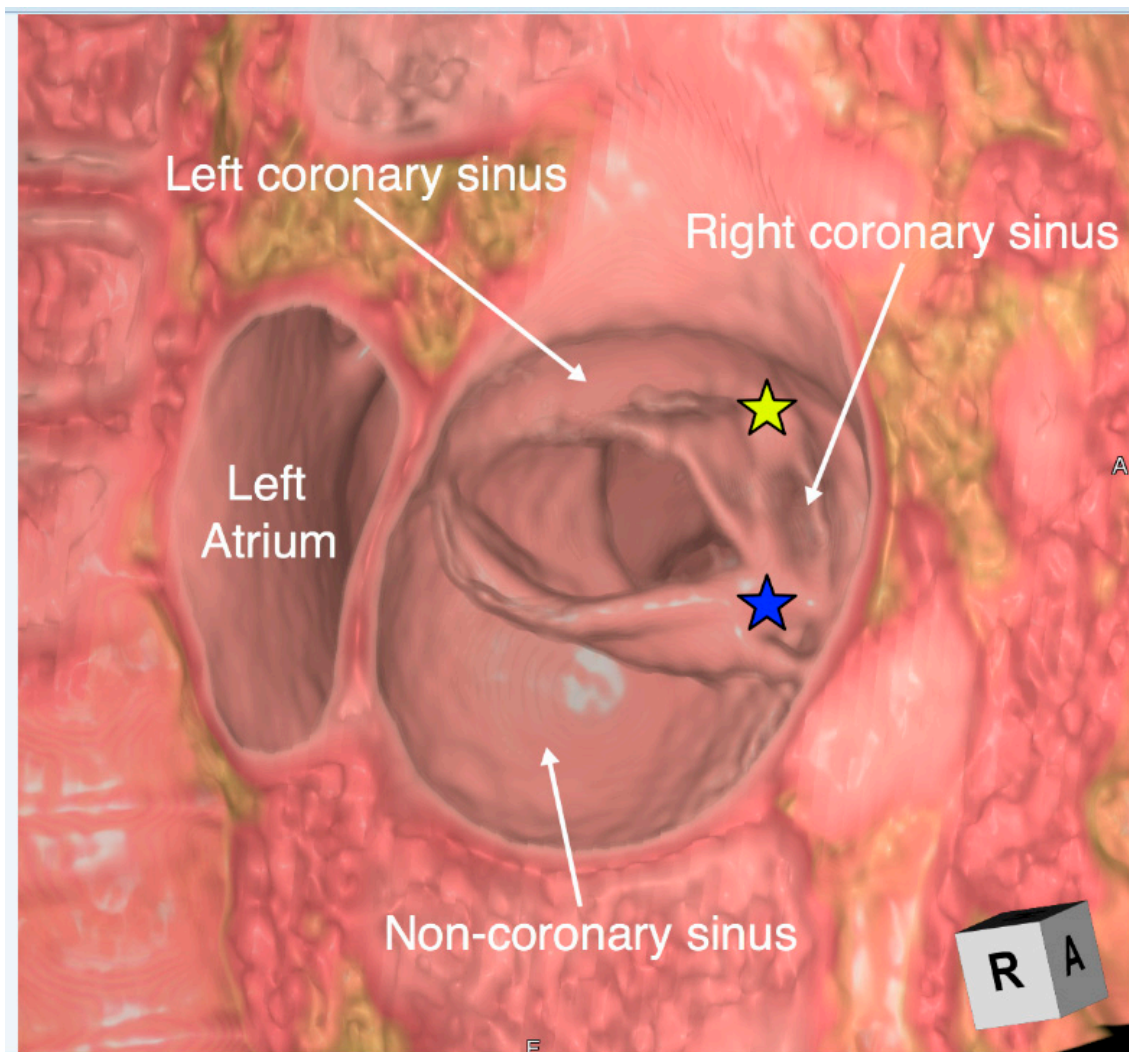


Figure 14. Virtual dissection of a unicuspid and unicommissural aortic valve viewed from the aorta. There is fusion with a raphe between both the right and left coronary leaflets (yellow star) and the right and non-coronary leaflets (blue star). A four-dimensional video is displayed in Supplemental Movie 2.

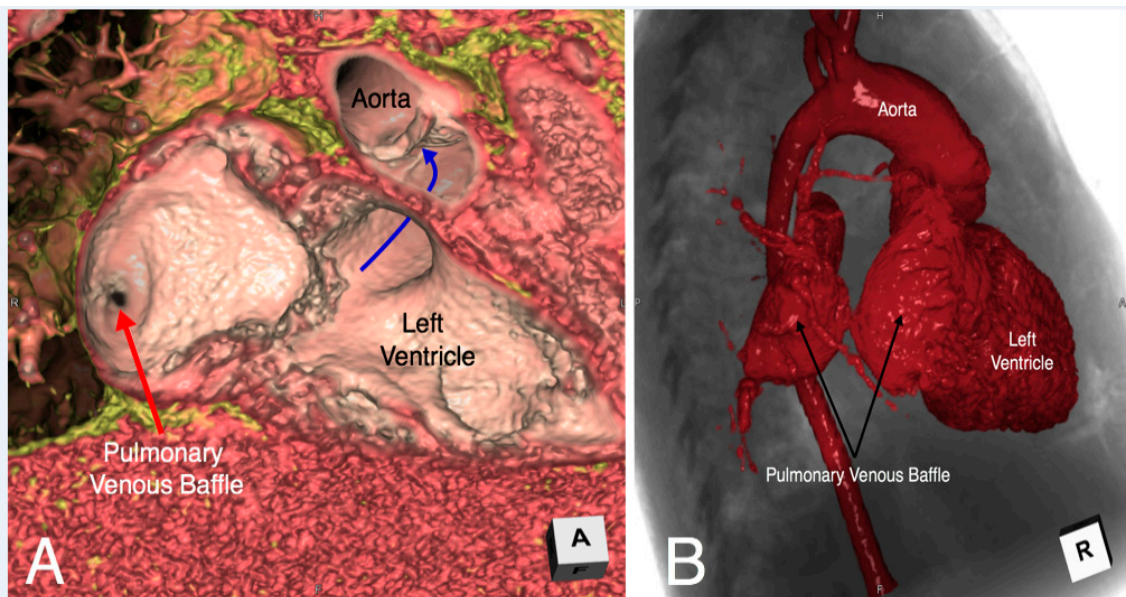


Figure 15. Virtual dissection (Panel A) and endocast reconstruction (Panel B) of a patient with congenitally corrected transposition status post double switch who developed severe obstruction of the pulmonary venous baffle. While the endocast image (Panel B) demonstrates the severe obstruction, it is the virtual dissection image (Panel A) which adds additional insight that the mechanism of obstruction is related to a membrane which has formed obstructing the pulmonary venous baffle.

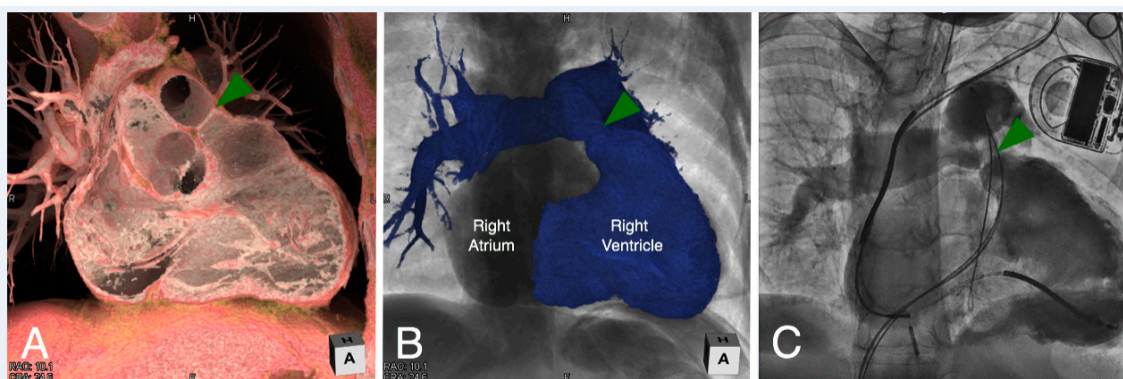


Figure 16. Virtual dissection (Panel A) and endocast reconstruction (Panel B) of a patient with repaired tetralogy of Fallot with moderate right ventricular outflow tract obstruction. Both images are viewed in a right anterior oblique plane. The virtual dissection image (Panel A) demonstrates a discrete ridge at the pulmonary sinutubular junction (green arrowhead). An angiogram was obtained in similar plane (Panel C) during cardiac catheterization confirming the anatomy, prior to placing a transcatheter pulmonary valve to relieve the obstruction.

7. Advanced Application of the Three-Dimensional Imaging

Three-dimensional imaging is currently used to create files for converting the image into three-dimensional printing [42] and virtual reality [33]. The printed model is useful for education as discussed above (Figure 17). Furthermore, it is also useful for surgeons for preoperational recognition of the complex anatomy, especially with the application of procedural simulation [12,43–45], as well as surgical training of the complicated procedures [46]. For this purpose, both endocast and virtual dissection images are used. Virtual reality supports the interactive sharing of the three-dimensional images during the simulated operation and also can guide the invasive procedures and operations, especially in such fields of orthopedics and neurosurgery [47,48]. As the heart is a highly moving

structure, the application of virtual reality into the clinical cardiovascular fields can be challenging. However, many groups are exploring this application [15,45]. Three-dimensional images, when combined with some software which has extended application equivalent to computer aided design, allow customization of the device by virtually simulating its shape and course (Figure 18) [49].

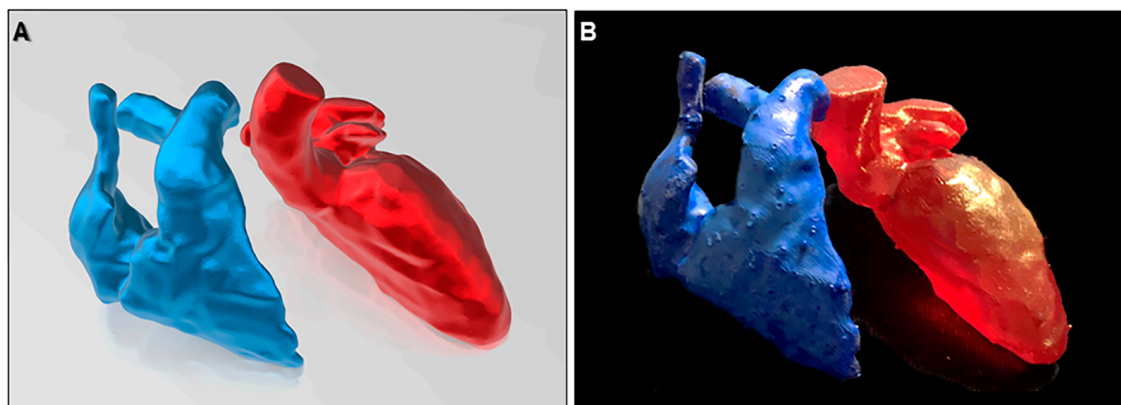


Figure 17. Virtual (A) and real (B) images of three-dimensional printing model of the right and left heart.

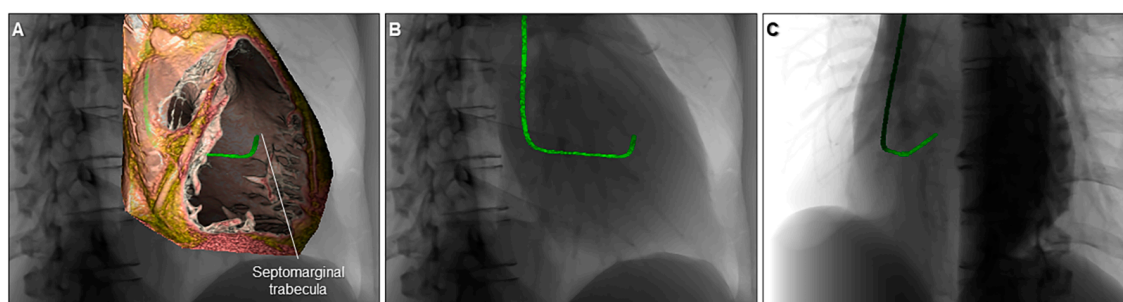


Figure 18. Virtual simulation of the catheter shape appropriate for right ventricular septal pacing visualized within the cardiac silhouette. The right ventricle is cut to show the septomarginal trabecula (A). The three-dimensional shape of the catheter is visualized in relation to the cardiac silhouette viewed from the right anterior oblique (B) and left anterior oblique (C) directions.

There is no doubt three-dimensional printed models and the increasing use of augmented and virtual reality can be extremely useful for education, procedural simulation and planning [12,43–45]. However, in our experience, utilizing the endocast and virtual dissection images on a monitor is often the most optimal strategy in clinical practice to provide a detailed evaluation of three-dimensional cardiac anatomy to support transcatheter and surgical planning while balancing costs and time efficiency [4,11,12,16,50,51]. Three-dimensional images in this paper were reconstructed using commercially available software/workstation (Horos, Pixmeo, Geneva, Switzerland; Ziostation2; Ziosoft, Tokyo, Japan; 3D Builder, Microsoft, Redmond, WA, USA).

Furthermore, for the analysis of cadaveric hearts, three-dimensional imaging plays an important role to clarify three-dimensional arrangement of the myocardial mesh and conduction system using diffusion tensor magnetic resonance imaging and microcomputed tomography [52,53].

8. Limitations of Three-Dimensional Imaging and Importance of Basic Anatomical Knowledge and Multidisciplinary Relationship

When creating three-dimensional images based on the volume-rendering method, it should be always kept in mind that the quality of the final image depends on the quality of the raw data. In this regard, the collaboration of radiologists and radiological technologists is an important prerequisite to

optimize image acquisition with appropriate radiation dose and contrast material [54]. While radiation exposure is a risk that must be weighed when considering alternative imaging options, with improving technology and the ability for minimal radiation exposure with modern scanners, the afforded spatial resolution has prompted increasing use of cardiac computed tomography [55].

The volume-rendered image might not precisely reflect the real anatomy. For example, the visualized anatomy can be enlarged or contracted from the real thing, depending on the software and window level/width applied. Thin or moving structures, such as the floor of the oval fossa (primary septum), membranous septum, and valvar leaflets are sometimes difficult to reconstruct, and can easily be mistaken for a defect. Some software can virtually create structures that are not present, such as vessels, as if it were a part of the real anatomy. Smoothing is commonly applied to some extent, which may distort the original information in the raw data. Therefore, measurements should not be performed on the volume-rendered image but should be measured using two-dimensional multiplanar reconstruction images. This can then be overlaid on the three-dimensional image for an improved understanding of these measurements related to the three-dimensional structure (Figure 19). Thus, to avoid creating images that can potentially mislead clinical judgement, it is paramount for the reconstructor to accurately interpret the anatomy based on the two-dimensional axial data [56]. It is the responsibility of the image creator to firmly visualize what can be seen in the raw data, and to acknowledge any structures which may be inaccurately demonstrated due to poor imaging quality. For this purpose, the most important basis for image reconstruction is the fundamental knowledge based on the real dissection-based anatomy, as we cannot visualize what we did not know [57]. Therefore, even if virtual dissection is considered the gold standard for anatomical analysis, as proposed by Professor Anderson [2], it is his achievements based on dissection-based cardiac anatomy that enables appropriate virtual dissection. Thus, virtual dissection can never completely replace the real dissection, but can surely provide complementary information relevant to educational and clinical management of patients with heart disease. Keeping good communication with radiologists, anatomists, clinical cardiologists, interventionalists, and surgeons is fundamental as these several departments are usually involved in the patient's care. These means of continuous multidisciplinary communication not only positively impact those performing procedures, but with constructive feedback to the imager relating the intraoperative findings to the provided reconstructions, also improve the quality and accuracy of reconstructions.

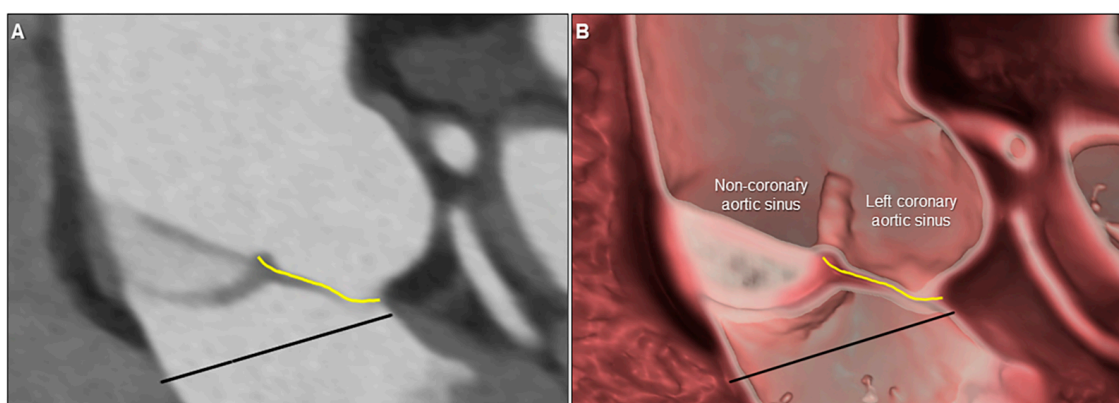


Figure 19. Two-dimensional multiplanar reconstruction (A) and three-dimensional virtual dissection (B) images showing the complicated anatomy of the aortic root. Yellow line and black line indicate geometric height and virtual basal ring plane, respectively. Measurement performed on the two-dimensional image can be projected on the three-dimensional image to secure the accuracy of the virtual dissection images.

9. Conclusions

The obtained three-dimensional data from each patient should be fully utilized to create images to show comprehensible clinical cardiac anatomy critical to the clinical diagnosis and treatment. In this

regard, virtual dissection, a three-dimensional volume-rendering imaging technique, is emerging as the gold standard for understanding detailed cardiac anatomy in the living patient. This technique is useful for both medical education as well as a detailed clinical evaluation of the complex three-dimensional heart, whether demonstrating normal anatomy for educational purposes or evaluating the patient with acquired or congenital heart disease. Any reconstruction depends both on the source imaging data as well as the anatomical understanding of the reconstructor. It is a requirement for radiologists, anatomists, cardiologists, interventionalists and surgeons to keep abreast of the benefits and limitations of these techniques and to fully utilize the three-dimensional anatomical data obtained to optimize patient management and outcomes.

Supplementary Materials: The following are available online at <http://www.mdpi.com/2308-3425/7/3/30/s1>, Supplementary Movie 1. Four-dimensional virtual dissection demonstrating the dynamic motion of the normal mitral valve throughout the cardiac cycle as viewed from the left atrium, Supplementary Movie 2. Four-dimensional virtual dissection demonstrating the dynamic motion of a unicuspid and unicommissural aortic valve. There is fusion with a raphe between both the right and left coronary leaflets and the right and non-coronary leaflets. The labeled image is displayed in Figure 14.

Author Contributions: Conceptualization, J.T.T., S.K.G., and S.M.; data acquisition and reconstruction of pediatric hearts, J.T.T. and S.K.G.; data acquisition and reconstruction of adult hearts, Y.I., T.N., and S.M.; validation, J.T.T., S.K.G., and S.M.; resources, J.T.T., S.K.G., Y.I., T.N., and S.M.; writing—original draft preparation, J.T.T. and S.M.; writing—review and editing, J.T.T., S.K.G., Y.I., T.N., and S.M.; radiological supervision, T.N.; overall supervision, S.M.; final revision and project administration, J.T.T. and S.M. All authors have read and agreed to the published version of the manuscript.

Funding: This research received no external funding.

Conflicts of Interest: The authors declare no conflict of interest.

References

1. Mori, S.; Tretter, J.T.; Spicer, D.E.; Bolender, D.L.; Anderson, R.H. What is the real cardiac anatomy? *Clin. Anat.* **2019**, *32*, 288–309. [[CrossRef](#)]
2. Anderson, R.H. Re-Setting the Gold Standard. *J. Cardiovasc. Electrophysiol.* **2015**, *26*, 713–714. [[CrossRef](#)]
3. Lin, E.; Alessio, A. What are the basic concepts of temporal, contrast, and spatial resolution in cardiac CT? *J. Cardiovasc. Comput. Tomogr.* **2009**, *3*, 403–408. [[CrossRef](#)]
4. Gupta, S.K.; Spicer, D.E.; Anderson, R.H. A new low-cost method of virtual cardiac dissection of computed tomographic datasets. *Ann. Pediatr. Cardiol.* **2019**, *12*, 110–116. [[CrossRef](#)]
5. Nagata, K.; Endo, S.; Honda, T.; Yasuda, T.; Hirayama, M.; Takahashi, S.; Kato, T.; Horita, S.; Furuya, K.; Kasai, K.; et al. Accuracy of CT Colonography for Detection of Polypoid and Nonpolypoid Neoplasia by Gastroenterologists and Radiologists: A Nationwide Multicenter Study in Japan. *Am. J. Gastroenterol.* **2017**, *112*, 163–171. [[CrossRef](#)]
6. Matsumoto, Y.; Izumo, T.; Sasada, S.; Tsuchida, T.; Ohe, Y. Diagnostic utility of endobronchial ultrasound with a guide sheath under the computed tomography workstation (ziostation) for small peripheral pulmonary lesions. *Clin. Respir. J.* **2017**, *11*, 185–192. [[CrossRef](#)]
7. Xu, X.; Zheng, Y.; Yao, S.; Sun, G.; Xu, B.; Chen, X. A low-cost multimodal head-mounted display system for neuroendoscopic surgery. *Brain Behav.* **2018**, *8*. [[CrossRef](#)] [[PubMed](#)]
8. Clifton, W.; Damon, A.; Valero-Moreno, F.; Nottmeier, E.; Pichelmann, M. The SpineBox: A Freely Available, Open-access, 3D-printed Simulator Design for Lumbar Pedicle Screw Placement. *Cureus* **2020**, *12*. [[CrossRef](#)]
9. Wada, K.; Arimoto, H.; Ohkawa, H.; Shirotani, T.; Matsushita, Y.; Takahara, T. Usefulness of preoperative three-dimensional computed tomographic angiography with two-dimensional computed tomographic imaging for rupture point detection of middle cerebral artery aneurysms. *Neurosurgery* **2008**, *62*, 126–132. [[CrossRef](#)] [[PubMed](#)]
10. Fukuzawa, K.; Nagamatsu, Y.; Mori, S.; Kiuchi, K.; Takami, M.; Izawa, Y.; Konishi, H.; Ichibori, H.; Imada, H.; Hyogo, K.; et al. Percutaneous Pericardiocentesis With the Anterior Approach: Demonstration of the Precise Course with Computed Tomography. *JACC Clin. Electrophysiol.* **2019**, *5*, 730–741. [[CrossRef](#)]

11. Steele, J.; Alsaied, T.; Crotty, E.J.; Tretter, J.T. Computed Tomographic 3-Dimensional Virtual Dissection Aiding Surgical Planning in a Rare Pediatric Case of Bicuspid Aortic Valve with Ascending Aorta Pseudoaneurysm. *Circ. Cardiovasc. Imaging* **2020**, *13*. [[CrossRef](#)] [[PubMed](#)]
12. McGovern, E.M.; Tretter, J.T.; Moore, R.A.; Goldstein, B.H. Simulation to Success: Treatment of a 3D printed heart before complex systemic venous baffle intervention. *JACC Case Rep.* **2020**, *2*, 486–487. [[CrossRef](#)]
13. Nishimori, M.; Kiuchi, K.; Mori, S.; Kurose, J.; Izawa, Y.; Kouno, S.; Nakagawa, H.; Shimoyama, S.; Fukuzawa, K.; Hirata, K.I. Atypical inferoseptal accessory pathway connection associated with an aneurysm of the coronary sinus: Insight from a three-dimensional combined image of electroanatomic mapping and computed tomography. *HeartRhythm Case Rep.* **2018**, *4*, 389–392. [[CrossRef](#)] [[PubMed](#)]
14. Vukicevic, M.; Mosadegh, B.; Min, J.K.; Little, S.H. Cardiac 3D Printing and its Future Directions. *JACC Cardiovasc. Imaging* **2017**, *10*, 171–184. [[CrossRef](#)] [[PubMed](#)]
15. Silva, J.N.A.; Southworth, M.; Raptis, C.; Silva, J. Emerging Applications of Virtual Reality in Cardiovascular Medicine. *JACC Basic Transl. Sci.* **2018**, *3*, 420–430. [[CrossRef](#)] [[PubMed](#)]
16. Schneider, K.; Ghaleb, S.; Morales, D.L.S.; Tretter, J.T. Virtual dissection and endocast three-dimensional reconstructions: Maximizing computed tomographic data for procedural planning of an obstructed pulmonary venous baffle. *Cardiol. Young* **2019**, *29*, 1104–1106. [[CrossRef](#)]
17. Mori, S.; Spicer, D.E.; Anderson, R.H. Revisiting the Anatomy of the Living Heart. *Circ. J.* **2016**, *80*, 24–33. [[CrossRef](#)]
18. Anderson, R.H.; Razavi, R.; Taylor, A.M. Cardiac anatomy revisited. *J. Anat.* **2004**, *205*, 159–177. [[CrossRef](#)]
19. Codreanu, A.; Odille, F.; Aliot, E.; Marie, P.Y.; Magnin-Poull, I.; Andronache, M.; Mandry, D.; Djaballah, W.; Régent, D.; Felblinger, J.; et al. Electroanatomic characterization of post-infarct scars comparison with 3-dimensional myocardial scar reconstruction based on magnetic resonance imaging. *J. Am. Coll. Cardiol.* **2008**, *52*, 839–842. [[CrossRef](#)]
20. Cochet, H.; Komatsu, Y.; Sacher, F.; Jadidi, A.S.; Scherr, D.; Riffaud, M.; Derval, N.; Shah, A.; Roten, L.; Pascale, P.; et al. Integration of merged delayed-enhanced magnetic resonance imaging and multidetector computed tomography for the guidance of ventricular tachycardia ablation: A pilot study. *J. Cardiovasc. Electrophysiol.* **2013**, *24*, 419–426. [[CrossRef](#)]
21. Mori, S.; Nishii, T.; Takaya, T.; Kashio, K.; Kasamatsu, A.; Takamine, S.; Ito, T.; Fujiwara, S.; Kono, A.K.; Hirata, K. Clinical structural anatomy of the inferior pyramidal space reconstructed from the living heart: Three-dimensional visualization using multidetector-row computed tomography. *Clin. Anat.* **2015**, *28*, 878–887. [[CrossRef](#)] [[PubMed](#)]
22. Mori, S.; Fukuzawa, K.; Takaya, T.; Takamine, S.; Ito, T.; Fujiwara, S.; Nishii, T.; Kono, A.K.; Yoshida, A.; Hirata, K. Clinical Structural Anatomy of the Inferior Pyramidal Space Reconstructed Within the Cardiac Contour Using Multidetector-Row Computed Tomography. *J. Cardiovasc. Electrophysiol.* **2015**, *26*, 705–712. [[CrossRef](#)] [[PubMed](#)]
23. Mori, S.; Fukuzawa, K.; Takaya, T.; Takamine, S.; Ito, T.; Fujiwara, S.; Nishii, T.; Kono, A.K.; Yoshida, A.; Hirata, K. Clinical cardiac structural anatomy reconstructed within the cardiac contour using multidetector-row computed tomography: Left ventricular outflow tract. *Clin. Anat.* **2016**, *29*, 353–363. [[CrossRef](#)] [[PubMed](#)]
24. Mori, S.; Fukuzawa, K.; Takaya, T.; Takamine, S.; Ito, T.; Fujiwara, S.; Nishii, T.; Kono, A.K.; Yoshida, A.; Hirata, K. Clinical cardiac structural anatomy reconstructed within the cardiac contour using multidetector-row computed tomography: Atrial septum and ventricular septum. *Clin. Anat.* **2016**, *29*, 342–352. [[CrossRef](#)]
25. Mori, S.; Fukuzawa, K.; Takaya, T.; Takamine, S.; Ito, T.; Fujiwara, S.; Nishii, T.; Kono, A.K.; Yoshida, A.; Hirata, K. Clinical cardiac structural anatomy reconstructed within the cardiac contour using multidetector-row computed tomography: The arrangement and location of the cardiac valves. *Clin. Anat.* **2016**, *29*, 364–370. [[CrossRef](#)]
26. Anderson, R.H.; Loukas, M. The importance of attitudinally appropriate description of cardiac anatomy. *Clin. Anat.* **2009**, *22*, 47–51. [[CrossRef](#)]
27. De Almeida, M.C.; Spicer, D.E.; Anderson, R.H. Why do we break one of the first rules of anatomy when describing the components of the heart? *Clin. Anat.* **2019**, *32*, 585–596. [[CrossRef](#)]
28. Ghosh, S.K. Cadaveric dissection as an educational tool for anatomical sciences in the 21st century. *Anat. Sci. Educ.* **2017**, *10*, 286–299. [[CrossRef](#)]

29. Ruzyccki, S.M.; Desy, J.R.; Lachman, N.; Wolanskyj-Spinner, A.P. Medical education for millennials: How anatomists are doing it right. *Clin. Anat.* **2019**, *32*, 20–25. [[CrossRef](#)]
30. Hołda, M.K.; Stefura, T.; Koziej, M.; Skomarowska, O.; Jasińska, K.A.; Sałabun, W.; Klimek-Piotrowska, W. Alarming decline in recognition of anatomical structures amongst medical students and physicians. *Ann. Anat.* **2019**, *221*, 48–56. [[CrossRef](#)]
31. Spitzer, V.M.; Scherzinger, A.L. Virtual anatomy: An anatomist's playground. *Clin. Anat.* **2006**, *19*, 192–203. [[CrossRef](#)] [[PubMed](#)]
32. Fonseca, C.G.; Backhaus, M.; Bluemke, D.A.; Britten, R.D.; Chung, J.D.; Cowan, B.R.; Dinov, I.D.; Finn, J.P.; Hunter, P.J.; Kadish, A.H.; et al. The Cardiac Atlas Project—An imaging database for computational modeling and statistical atlases of the heart. *Bioinformatics* **2011**, *27*, 2288–2295. [[CrossRef](#)] [[PubMed](#)]
33. Maresky, H.S.; Oikonomou, A.; Ali, I.; Ditkofsky, N.; Pakkal, M.; Ballyk, B. Virtual reality and cardiac anatomy: Exploring immersive three-dimensional cardiac imaging, a pilot study in undergraduate medical anatomy education. *Clin. Anat.* **2019**, *32*, 238–243. [[CrossRef](#)] [[PubMed](#)]
34. Tretter, J.T.; Mori, S. Two-Dimensional Imaging of a Complex Three-Dimensional Structure: Measurements of Aortic Root Dimensions. *J. Am. Soc. Echocardiogr.* **2019**, *32*, 792–794. [[CrossRef](#)] [[PubMed](#)]
35. Baskar, S.; Gray, S.B.; Del Grippo, E.L.; Osakwe, O.; Powell, A.W.; Tretter, J.T. Cardiac morphology for the millennial cardiology fellow: Nomenclature and advances in morphologic imaging. *Congenit. Heart Dis.* **2018**, *13*, 808–810. [[CrossRef](#)]
36. Hasegawa, K.; Takaya, T.; Mori, S.; Ito, T.; Fujiwara, S.; Nishii, T.; Kono, A.K.; Shimoura, H.; Tanaka, H.; Hirata, K.I. Compression of the Right Ventricular Outflow Tract due to Straight Back Syndrome Clarified by Low-dose Dual-source Computed Tomography. *Intern. Med.* **2016**, *55*, 3279–3283. [[CrossRef](#)]
37. Ichibori, H.; Mori, S.; Takaya, T.; Kiuchi, K.; Ito, T.; Fujiwara, S.; Fukuzawa, K.; Tatsumi, K.; Tanaka, H.; Nishii, T.; et al. Slit-Like Deformation of the Coronary Sinus Orifice due to Compression of the Inferior Pyramidal Space by the Severely Dilated Left Ventricle. *Pacing Clin. Electrophysiol.* **2016**, *39*, 1026–1029. [[CrossRef](#)]
38. Konishi, H.; Mori, S.; Nishii, T.; Izawa, Y.; Tamada, N.; Tanaka, H.; Kiuchi, K.; Fukuzawa, K.; Hirata, K.I. Extracardiac compression of the inferolateral branch of the coronary vein by the descending aorta in a patient with dilated cardiomyopathy. *J. Arrhythm.* **2017**, *33*, 646–648. [[CrossRef](#)]
39. Izawa, Y.; Mori, S.; Nishii, T.; Matsuzoe, H.; Imada, H.; Suehiro, H.; Nakayama, K.; Matsumoto, K.; Tanaka, H.; Fujiwara, S.; et al. Optimal image reconstruction using multidetector-row computed tomography to facilitate cardiac resynchronization therapy. *Echocardiography* **2017**, *34*, 1073–1076. [[CrossRef](#)]
40. Toh, H.; Mori, S.; Shimoyama, S.; Izawa, Y.; Yokota, S.; Shinkura, Y.; Takeshige, R.; Nagasawa, A.; Soga, F.; Tanaka, H.; et al. Optimal reconstruction of left ventricular outflow tract obstruction before surgical myectomy in a case with hypertrophic obstructive cardiomyopathy. *Echocardiography* **2018**, *35*, 537–540. [[CrossRef](#)]
41. Burchill, L.J.; Huang, J.; Tretter, J.T.; Khan, A.M.; Crean, A.M.; Veldtman, G.R.; Kaul, S.; Broberg, C.S. Noninvasive Imaging in Adult Congenital Heart Disease. *Circ. Res.* **2017**, *120*, 995–1014. [[CrossRef](#)] [[PubMed](#)]
42. Costello, J.P.; Olivieri, L.J.; Krieger, A.; Thabit, O.; Marshall, M.B.; Yoo, S.J.; Kim, P.C.; Jonas, R.A.; Nath, D.S. Utilizing Three-Dimensional Printing Technology to Assess the Feasibility of High-Fidelity Synthetic Ventricular Septal Defect Models for Simulation in Medical Education. *World J. Pediatr. Congenit. Heart Surg.* **2014**, *5*, 421–426. [[CrossRef](#)] [[PubMed](#)]
43. Bhatla, P.; Tretter, J.T.; Ludomirsky, A.; Argilla, M.; Latson, L.A.; Chakravarti, S., Jr.; Barker, P.C.; Yoo, S.J.; McElhinney, D.B.; Wake, N.; et al. Utility and Scope of Rapid Prototyping in Patients with Complex Muscular Ventricular Septal Defects or Double-Outlet Right Ventricle: Does it Alter Management Decisions? *Pediatr. Cardiol.* **2017**, *38*, 103–114. [[CrossRef](#)] [[PubMed](#)]
44. Bhatla, P.; Tretter, J.T.; Chikkabyrappa, S.; Chakravarti, S.; Mosca, R.S. Surgical planning for a complex double-outlet right ventricle using 3D printing. *Echocardiography* **2017**, *34*, 802–804. [[CrossRef](#)]
45. Moore, R.A.; Riggs, K.W.; Kourtidou, S.; Schneider, K.; Szugye, N.; Troja, W.; D'Souza, G.; Rattan, M.; Bryant, R.; Taylor, M.D., III; et al. Three-dimensional printing and virtual surgery for congenital heart procedural planning. *Birth Defects Res.* **2018**, *110*, 1082–1090. [[CrossRef](#)]
46. Yoo, S.J.; Spray, T.; Austin, E.H.; Yun, T.J., III; van Arsdell, G.S. Hands-on surgical training of congenital heart surgery using 3-dimensional print models. *J. Thorac. Cardiovasc. Surg.* **2017**, *153*, 1530–1540. [[CrossRef](#)]

47. Jud, L.; Fotouhi, J.; Andronic, O.; Aichmair, A.; Osgood, G.; Navab, N.; Farshad, M. Applicability of augmented reality in orthopedic surgery—A systematic review. *BMC Musculoskelet. Disord.* **2020**, *21*, 103. [[CrossRef](#)]
48. Elmi-Terander, A.; Burström, G.; Nachabé, R.; Fagerlund, M.; Ståhl, F.; Charalampidis, A.; Edström, E.; Gerdhem, P. Augmented reality navigation with intraoperative 3D imaging vs. fluoroscopy-assisted free-hand surgery for spine fixation surgery: A matched-control study comparing accuracy. *Sci. Rep.* **2020**, *10*, 707. [[CrossRef](#)]
49. Kasamatsu, A.; Takaya, T.; Mori, S.; Kashio, K.; Takahashi, H.; Ito, T.; Takamine, S.; Fujiwara, S.; Nishii, T.; Kono, A.K.; et al. Reconstruction of an extracardiac aortocoronary collateral and simulation of selective angiography with multidetector-row computed tomography. *Circulation* **2015**, *131*, 476–479. [[CrossRef](#)]
50. Gupta, S.K.; Anderson, R.H. Virtual dissection: An alternative to surface-rendered virtual three-dimensional cardiac model. *Ann. Pediatr. Cardiol.* **2020**, *13*, 102–103. [[CrossRef](#)]
51. Sachdeva, S.; Gupta, S.K. Imaging Modalities in Congenital Heart Disease. *Indian J. Pediatr.* **2020**, *87*, 385–397. [[CrossRef](#)] [[PubMed](#)]
52. Stephenson, R.S.; Agger, P.; Omann, C.; Sanchez-Quintana, D.; Jarvis, J.C.; Anderson, R.H. Resolving the True Ventricular Mural Architecture. *J. Cardiovasc. Dev. Dis.* **2018**, *5*, 34. [[CrossRef](#)] [[PubMed](#)]
53. Stephenson, R.S.; Atkinson, A.; Kottas, P.; Perde, F.; Jafarzadeh, F.; Bateman, M.; Iaizzo, P.A.; Zhao, J.; Zhang, H.; Anderson, R.H.; et al. High resolution 3-Dimensional imaging of the human cardiac conduction system from microanatomy to mathematical modeling. *Sci. Rep.* **2017**, *7*, 7188. [[CrossRef](#)] [[PubMed](#)]
54. Nishii, T.; Watanabe, Y.; Shimoyama, S.; Kono, A.K.; Sofue, K.; Mori, S.; Takahashi, S.; Sugimura, K. Tailored Duration of Contrast Material Injection in High-Pitch Computed Tomographic Aortography With a Double-Level Test Bolus Method. *Invest. Radiol.* **2017**, *52*, 274–280. [[CrossRef](#)]
55. Han, B.K.; Rigsby, C.K.; Hlavacek, A.; Leipsic, J.; Nicol, E.D.; Siegel, M.J.; Bardo, D.; Abbara, S.; Ghoshhajra, B.; Lesser, J.R.; et al. Computed Tomography Imaging in Patients with Congenital Heart Disease Part I: Rationale and Utility. An Expert Consensus Document of the Society of Cardiovascular Computed Tomography (SCCT): Endorsed by the Society of Pediatric Radiology (SPR) and the North American Society of Cardiac Imaging (NASCI). *J. Cardiovasc. Comput. Tomogr.* **2015**, *9*, 475–492.
56. Anderson, R.H.; Bolender, D.; Mori, S.; Tretter, J.T. Virtual Reality Perhaps, but Is this Real Cardiac Anatomy? *Clin. Anat.* **2019**, *32*, 468. [[CrossRef](#)]
57. Bradfield, J.S.; Fujimura, O.; Boyle, N.G.; Shivkumar, K. Catheter ablation in the vicinity of the proximal conduction system: Your eyes cannot see what your mind does not know. *Heart Rhythm* **2019**, *16*, 378–379. [[CrossRef](#)]

